

Thermal decomposition of some alkali-metal–bromobismuthate(III) complexes

Bogdan Ptaszyński

Institute of General and Ecological Chemistry, Polytechnical University, 90924 Łódź (Poland)

(Received 24 June 1991)

Abstract

Thermal decomposition of crystalline complex salts $\text{Na}_2[\text{BiBr}_5] \cdot 4\text{H}_2\text{O}$, $\text{Na}_3[\text{BiBr}_6] \cdot 12\text{H}_2\text{O}$, $\text{K}_4[\text{Bi}_2\text{Br}_{10}] \cdot 4\text{H}_2\text{O}$, $\text{Rb}_3[\text{BiBr}_6]$ and $\text{Cs}_3[\text{Bi}_2\text{Br}_9]$ has been studied. On the basis of thermal analysis, X-ray and chemical analyses of their decomposition products thermal decomposition reactions have been established. From thermogravimetric curves kinetic parameters are calculated using the methods of Coats–Redfern and Zsako.

INTRODUCTION

The present work is a continuation of our studies on thermal decomposition of crystalline halogenide complexes of arsenic(III), antimony(III) and bismuth(III) by thermal, chemical and X-ray analyses [1–7]. The earlier papers on alkali-metal–bromobismuthate(III) complexes were mainly concerned with methods of preparation [8–12] and structural studies [13–14] of these compounds. Some information on their thermal stability was also published [16–18] but mechanisms of thermal decomposition in dynamic conditions have not been examined in detail. Kinetic parameters of decomposition reactions of bromobismuthate(III) complexes have not so far been evaluated.

EXPERIMENTAL

Apparatus

Thermal analysis was carried out in air using a MOM Budapest OD 102/1500°C thermal analyser over a temperature range 20–1000°C at a heating of 5°C min⁻¹. The sample mass was 100 mg. $\alpha\text{-Al}_2\text{O}_3$ was used as reference material. The sensitivity of the galvanometer for the DTA curves was 1/5 and for the DTG curves 1/15.

Correspondence to: B. Ptaszyński, Institute of General and Ecological Chemistry, Polytechnical University, 90924 Łódź, Poland.

X-Ray analyses were carried out on a DRON-1 diffractometer using Cu $K\alpha$ radiation with a nickel filter. Diffracted rays were recorded over the 2θ range 2–60°.

Preparation of bromobismuthate(III) complexes

Crystals of alkali-metal–bromobismuthate(III) complexes were prepared by dissolving M_2CO_3 or MBr (M = alkali metal) and $(BiO)_2CO_3 \cdot 0.5 H_2O$ at different molar proportions $M:Bi$ in excess of 20% hydrobromic acid, followed by slow evaporation of the solutions at room temperature. Crystals were dried in air and analysed. Bismuth was determined as sulfide by precipitating it with thioacetamide and bromide by Volhard's method [19].

In the system $NaBr-BiBr_3-HBr-H_2O$ at the molar proportion $Na:Bi = 1:1$ after about two weeks a mixture of $Na_2[BiBr_5] \cdot 4H_2O$ and $Na_3[BiBr_6] \cdot 12H_2O$ separated whereas at $Na:Br = 2:1$ $Na_2[BiBr_5] \cdot 4H_2O$ crystallised.

In the system $KBr-BiBr_3-HBr-H_2O$ at molar proportion $K:Bi = 3:1$, as a result of very slow crystallisation, a mixture of yellow crystals of $K_4[Bi_2Br_{10}] \cdot 4H_2O$ and KBr was obtained.

In the case of rubidium and caesium compounds at $M:Bi = 2:1$ and $3:1$ ($M = Rb, Cs$) anhydrous salts of formulae $Rb_3[BiBr_6]$ and $Cs_3[Bi_2Br_9]$ crystallised. Fine crystals of caesium bromobismuthate instantly separated

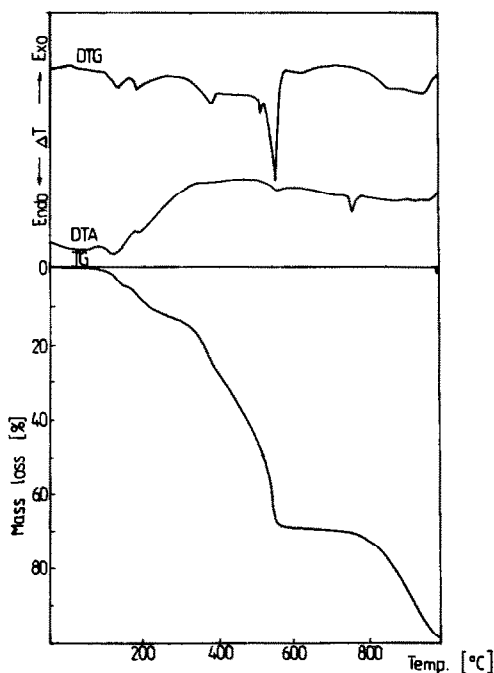


Fig. 1. Thermal curves of $Na_2[BiBr_5] \cdot 4H_2O$.

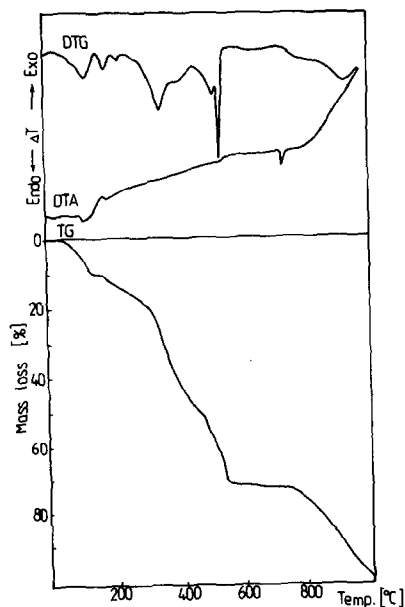


Fig. 2. Thermal curves of $\text{Na}_3[\text{BiBr}_6] \cdot 12\text{H}_2\text{O}$.

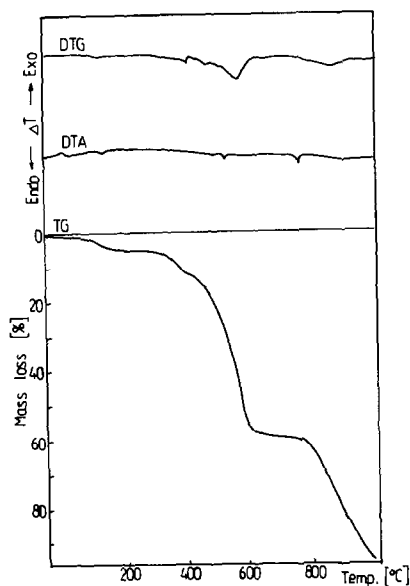


Fig. 3. Thermal curves of $\text{K}_4[\text{Bi}_2\text{Br}_{10}] \cdot 4\text{H}_2\text{O}$.

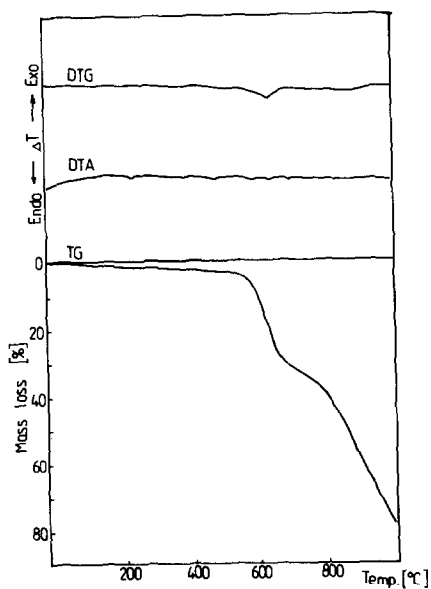


Fig. 4. Thermal curves of $\text{Rb}_3[\text{BiBr}_6]$.

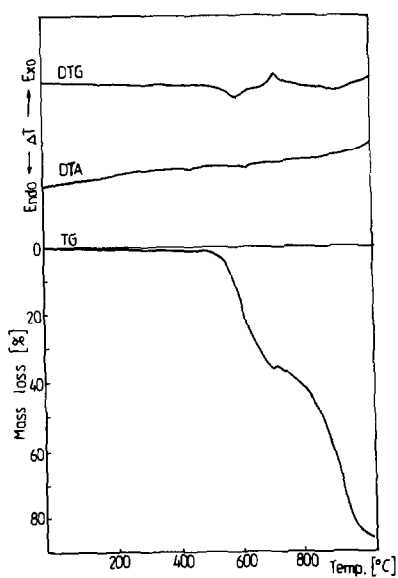


Fig. 5. Thermal curves of $\text{Cs}_3[\text{Bi}_2\text{Br}_9]$.

TABLE 1

Thermal decomposition data

Compound	Stage of decomposition	Temperature range of decomposition (°C)	DTA peak temperature (°C)
$\text{Na}_2[\text{BiBr}_5] \cdot 4\text{H}_2\text{O}$	I	70–145	110
	II	150–200	172
	III } IV }	200–545	370, 545, 746
$\text{Na}_3[\text{BiBr}_6] \cdot 12\text{H}_2\text{O}$	I	60–170	110
	II	170–320	180
	III	320–450	350
	IV	450–550	540, 746
$\text{K}_4[\text{Bi}_2\text{Br}_{10}] \cdot 4\text{H}_2\text{O}$	I	100–190	136
	II } III }	270–660	460, 510, 740
$\text{Rb}_3[\text{BiBr}_6]$	I	500–690	465, 584
	II	690–900	630
$\text{Cs}_3[\text{Bi}_2\text{Br}_9]$	I	500–700	620
	II	700–900	

from the solution whereas crystals of the rubidium salt appeared after about two weeks.

Attempts to prepare crystalline lithium bromobismuthate(III) failed.

Analysis of thermal curves

The thermal analysis curves of alkali-metal–bromobismuthate(III) complexes are shown in Figs. 1–5 and concise thermoanalytical data are presented in Table 1. The analysis of TG, DTA and DTG curves of $\text{Na}_2[\text{BiBr}_5] \cdot 4\text{H}_2\text{O}$ (Fig. 1) suggests a four-step decomposition of this compound which takes place within the range 90–560°C. The first stage (90–145°C) is connected with the loss of 2 moles of water (the observed 5% decrease in mass on TG is in good accord with the theoretical value of 4.96%). In the second stage (150 to about 200°C) the remaining water is removed. The corresponding diffuse peaks on DTG are at 110 and 172°C, respectively. The next stages overlap and at 550°C the decomposition of $\text{Na}_2[\text{BiBr}_5] \cdot 4\text{H}_2\text{O}$ is complete. The only sharp endothermic peak on the DTA curve at 746°C corresponds to the melting of NaBr (m.p. 746.8°C). The mass decrement observed on the TG curve above 750°C is connected with the evaporation of molten sodium bromide.

According to the thermoanalytical curves (Fig. 2) $\text{Na}_3[\text{BiBr}_6] \cdot 12\text{H}_2\text{O}$ undergoes a four-step decomposition within the range 60–650°C. In the

first stage, which takes place between 60 and 170°C, the mass loss determined from TG (11%) is in good agreement with that calculated for the removal of 6 moles of water (11.09%). The corresponding peak on DTA is at 104°C. The second stage of decomposition begins at 170°C and finishes at about 320°C and is connected with the loss of the remaining six moles of water. The appropriate endothermic peak on DTA is at 173°C. The subsequent stages overlap and their temperature limits cannot be precisely determined. The corresponding peaks on DTA are small and diffuse and have maxima at 347 and 538°C, respectively. The sharp endothermic peak on DTA at 740°C corresponds to the melting of sodium bromide. Above this temperature the slow evaporation of NaBr takes place.

The course of the thermoanalytical curves of $K_4[Bi_2Br_{10}] \cdot 4H_2O$ (Fig. 3) indicates a three-step decomposition. In the first stage (100–190°C) the loss of mass on TG (5%) corresponds to the removal of water of crystallisation. The appropriate peak on DTA is at 136°C. The decomposition of the anhydrous salt starts at 270°C. The second and third stages partly overlap; their approximate ranges are 250–400°C and 400–600°C, respectively. The corresponding peaks on DTA are at 460°C (small, diffuse) and 510°C (sharp). The sharp peak on DTA at 740°C is connected with the melting of potassium bromide (m.p. KBr, 741°C).

The approximate course of reaction of thermal decomposition of $Rb_3[BiBr_6]$ has been previously determined [2]. The actual study was carried out under slightly different experimental conditions. According to

TABLE 2

Temperatures of sinter preparation and bismuth content in sinters

Compound	Temperature (°C)	Loss of mass (%)		Bi content (%)
		Weighted	From TG	
$Na_2[BiBr_5] \cdot 4H_2O$	180	10.1	9.5	31.1
	360	21.7	24.0	20.37
	550	68.3	69.0	1.89
	810	72.2	74.0	0.0
$Na_3[BiBr_6] \cdot 12H_2O$	200	13.9	13.5	23.1
	340	26.2	27.4	19.04
	530	68.3	66.2	1.94
	770	73.2	74.5	0.0
$K_4[Bi_2Br_{10}] \cdot 4H_2O$	400	12.6	12.0	23.46
	500	25.5	28.0	15.57
	850	68.8	71.0	0,0
$Rb_3[BiBr_6]$	900	57.6	55.3	1.12
$Cs_3[Bi_2Br_9]$	800	41.9	40.0	0.86

the thermoanalytical curves (Fig. 4) rubidium hexabromobismuthate(III) decomposes probably in two stages in rapid succession. Its thermal stability is distinctly higher than sodium and potassium salts. The slow and slight mass decrement ($< 3\%$) observed on TG up to about 500°C is connected with the removal of hygroscopic water and volatile surface impurities. The decomposition reaction starts at about 500°C and is complete at about 900°C . The inflection point on TG at 690°C probably corresponds to the end of the first step and simultaneously to the beginning of the second step of the decomposition reaction. The approximate loss of mass of both stages on TG is equal to 28% . The DTA curve exhibits several small but distinct endothermic peaks. The first, at 465°C , not accompanied by the mass decrement is connected with the phase change of the parent compound. It was confirmed by X-ray analysis. The second peak at 584°C corresponds to the melting of $\text{Rb}_3[\text{BiBr}_6]$. The next peak at 630°C is connected with the first stage of decomposition of the compound under study while at 685°C corresponds to the melting of rubidium bromide being the final product of

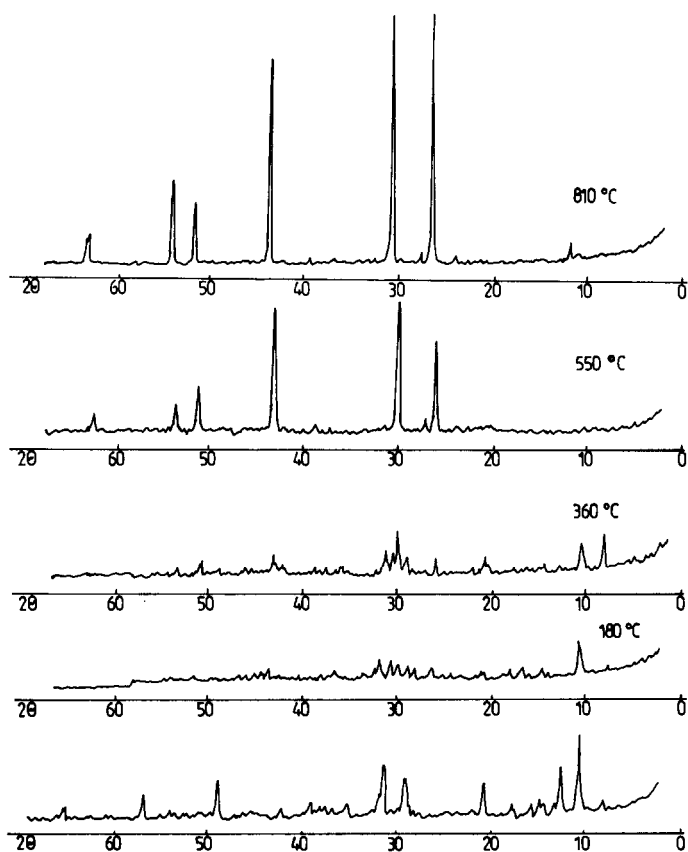


Fig. 6. X-Ray diffraction patterns of $\text{Na}_2[\text{BiBr}_5] \cdot 4\text{H}_2\text{O}$ and sinters.

decomposition (m.p. RbBr, 677°C). The rapid mass decrement observed on TG above 900°C is connected with the evaporation of the molten RbBr.

Thermal curves of $\text{Cs}_3[\text{Bi}_2\text{Br}_9]$ (Fig. 5) are almost identical with those published earlier [2,12], the peaks on DTA and DTG being displaced towards lower temperatures by about 10°C, probably as a result of the slower heating rate. The only sharp endothermic peak on DTA at 620°C corresponds to the melting of Cs_3BiBr_6 (the intermediate product of decomposition of $\text{Cs}_3[\text{Bi}_2\text{Br}_9]$). The first stage of reaction takes place within the range 500–700°C. The mass decrement of the second stage (> 700°C) is a consequence of simultaneous processes of decomposition of $\text{Cs}_3[\text{Bi}_2\text{Br}_9]$ and evaporation of molten caesium bromide (m.p. CsBr, 636°C).

Preparation and chemical analyses of sinters

In order to study the course of decomposition reactions sinters were prepared under conditions similar to those used in the thermal analysis.

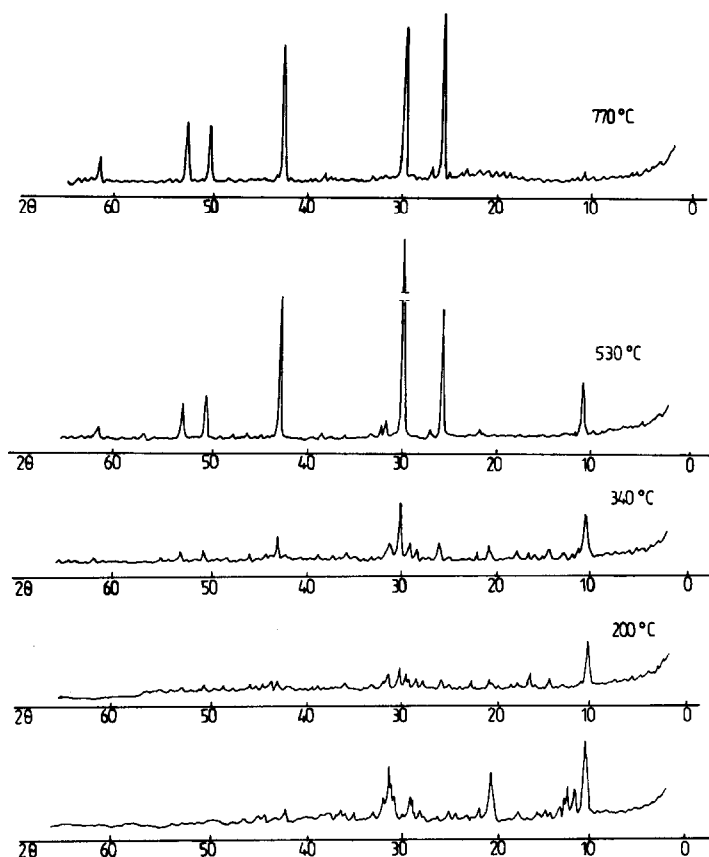


Fig. 7. X-Ray diffraction patterns of $\text{Na}_3[\text{BiBr}_6] \cdot 12\text{H}_2\text{O}$ and sinters.

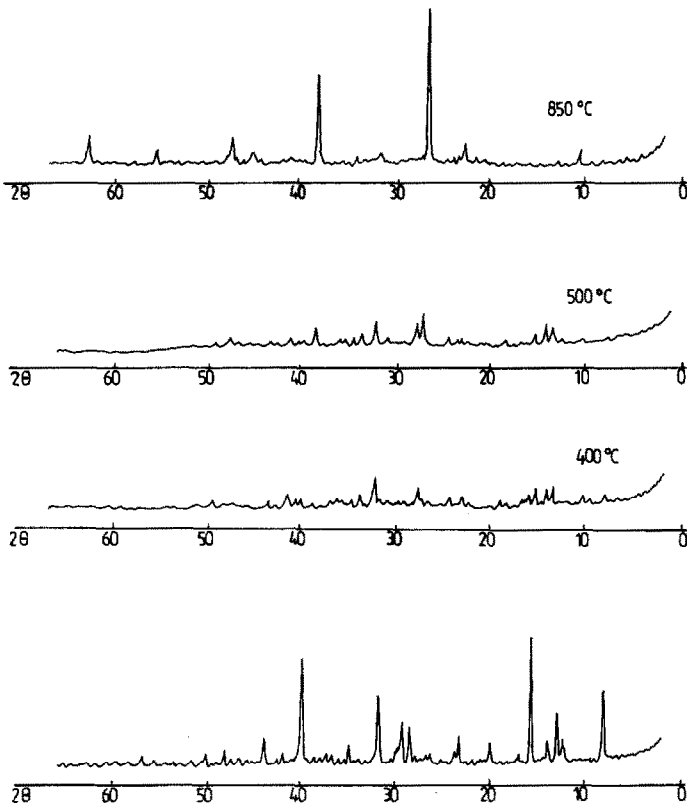


Fig. 8. X-Ray diffraction patterns of $\text{K}_4[\text{Bi}_2\text{Br}_{10}] \cdot 4\text{H}_2\text{O}$ and sinters.

“Sinter” means solid intermediate or final product of decomposition. Samples of bromobismuthates of 100 mg were heated in an electric silitite furnace at a heating rate of about 5°C min^{-1} up to the temperatures

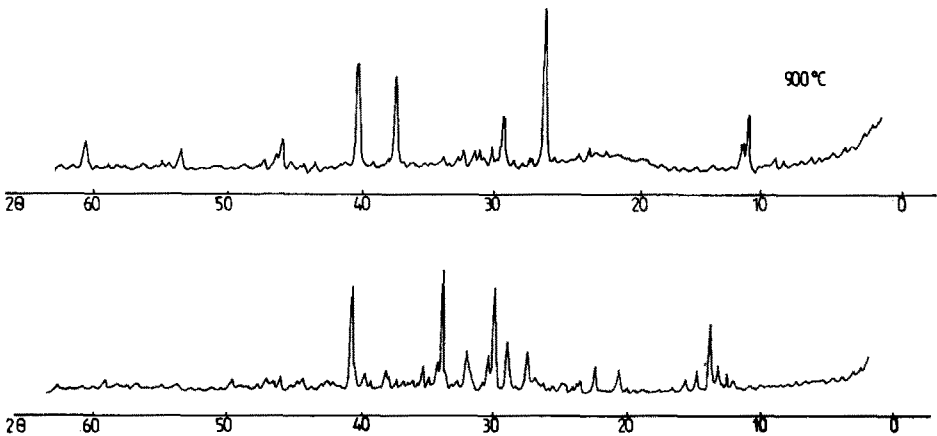


Fig. 9. X-Ray diffraction patterns of $\text{Rb}_3[\text{BiBr}_6]$ and sinters.

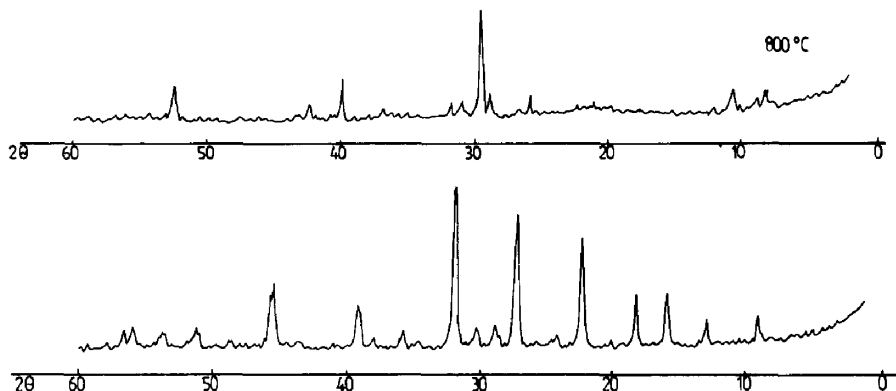


Fig. 10. X-Ray diffraction patterns of $\text{Cs}_3[\text{Bi}_2\text{Br}_9]$ and sinters.

corresponding to the end of the particular stages of reactions and also to the temperatures at which the decomposition was complete. For further investigations sinters which showed the loss of mass identical with or similar to those evaluated from TG were taken (Table 2). In sinters bismuth was determined gravimetrically as sulfide by precipitating it with thioacetamide.

X-ray analysis

For each compound under study X-ray diffraction patterns of the original compound as well as of sinters prepared at appropriate temperatures (Table 2) were obtained. The results are presented at Figs. 6–10. The sinters exhibit entirely different patterns from those obtained for the parent compounds. Both intermediate and final products of decomposition constitute a crystalline phase. The patterns of sinters obtained at high temperatures exhibit exclusively peaks characteristic for the appropriate alkali metal bromide. The presence of these peaks on the X-ray diffraction patterns of the intermediate products of decomposition was also established. The higher the temperature at which a sinter was prepared the higher were the peaks characteristic for alkali metal bromide. The X-ray diffraction pattern of $\text{Na}_2[\text{BiBr}_5] \cdot 4\text{H}_2\text{O}$ heated to 180°C is similar to that of $\text{Na}_3[\text{BiBr}_6] \cdot 12\text{H}_2\text{O}$ sinter obtained at 200°C suggesting the same intermediate product of the first stage of decomposition of both compounds.

CONCLUSIONS

During the thermal decomposition of alkali-metal–bromobismuthate(III) complexes, gaseous BiBr_3 is liberated. The intermediate and final products of the reactions constitute a crystalline phase. All thermal effects on DTA

curves are endothermic. The melting points of alkali metal bromides determined from DTA differ slightly from correct melting point data. According to the results of thermal, chemical and X-ray analyses of the intermediate and final products of these reactions, the thermal decomposition of alkali-metal-bromobismuthate(III) complexes are multi-step processes which can be supposed to proceed according to the following schemes.

For $\text{Na}_2[\text{BiBr}_5] \cdot 4\text{H}_2\text{O}$

step I (70–145°C) $\text{Na}_2[\text{BiBr}_5] \cdot 4\text{H}_2\text{O} = \text{Na}_2[\text{BiBr}_5] \cdot 2\text{H}_2\text{O} + 2\text{H}_2\text{O}$

step II (150–200°C) $\text{Na}_2[\text{BiBr}_5] \cdot 2\text{H}_2\text{O} = \text{Na}_2[\text{BiBr}_5] + 2\text{H}_2\text{O}$

step III (200–?°C) $2\text{Na}_2[\text{BiBr}_5] = \text{Na}_4[\text{BiBr}_7] + \text{BiBr}_3$

step IV (?–545°C) $\text{Na}_4[\text{BiBr}_7] = 4\text{NaBr} + \text{BiBr}_3$

For $\text{Na}_3[\text{BiBr}_6] \cdot 12\text{H}_2\text{O}$

step I (60–170°C) $\text{Na}_3[\text{BiBr}_6] \cdot 12\text{H}_2\text{O} = \text{Na}_3[\text{BiBr}_6] \cdot 6\text{H}_2\text{O} + 6\text{H}_2\text{O}$

step II (170–320°C) $\text{Na}_3[\text{BiBr}_6] \cdot 6\text{H}_2\text{O} = \text{Na}_2[\text{BiBr}_5] + \text{NaBr} + 6\text{H}_2\text{O}$

step III (320–450°C) $2\text{Na}_2[\text{BiBr}_5] = \text{Na}_4[\text{BiBr}_7] + \text{BiBr}_3$

step IV (450–550°C) $\text{Na}_4[\text{BiBr}_7] = 4\text{NaBr} + \text{BiBr}_3$

For $\text{K}_4[\text{Bi}_2\text{Br}_{10}] \cdot 4\text{H}_2\text{O}$

step I (100–190°C) $\text{K}_4[\text{Bi}_2\text{Br}_{10}] \cdot 4\text{H}_2\text{O} = 2\text{K}_2[\text{BiBr}_5] + 4\text{H}_2\text{O}$

step II (270–450°C) $2\text{K}_2[\text{BiBr}_5] = \text{K}[\text{BiBr}_4] + 3\text{KBr} + \text{BiBr}_3$

step III (450–660°C) $\text{K}[\text{BiBr}_4] = \text{KBr} + \text{BiBr}_3$

For $\text{Rb}_3[\text{BiBr}_6]$

step I (500–690°C) $2\text{Rb}_3[\text{BiBr}_6] = \text{Rb}_2[\text{BiBr}_5] + 4\text{RbBr} + \text{BiBr}_3$

step II (690–950°C) $\text{Rb}_2[\text{BiBr}_5] = 2\text{RbBr} + \text{BiBr}_3$

For $\text{Cs}_3[\text{Bi}_2\text{Br}_9]$

step I (500–700°C) $\text{Cs}_3[\text{Bi}_2\text{Br}_9] = \text{Cs}_3[\text{BiBr}_6] + \text{BiBr}_3$

step II (700–900°C) $\text{Cs}_3[\text{BiBr}_6] = 3\text{CsBr} + \text{BiBr}_3$

These equations are idealised. In reality some steps of reactions partly overlap, so it is difficult to determine the exact temperature ranges of the individual reaction stages.

Activation energies and reaction orders of some steps of decomposition reactions were calculated from TG curves using the Coats–Redfern and Zsako methods. The final results are presented in Table 3.

The thermal stability of compounds under study, defined by the temperature at which the decomposition starts and also by the temperature of the endothermic peak on the DTA curve corresponding to the first step of decomposition, increase distinctly in the order $\text{Na}_2[\text{BiBr}_5] \cdot 4\text{H}_2\text{O} \approx \text{Na}_3[\text{BiBr}_6] \cdot 12\text{H}_2\text{O} < \text{K}_4[\text{Bi}_2\text{Br}_{10}] \cdot 4\text{H}_2\text{O} \ll \text{Rb}_3[\text{BiBr}_6] \approx \text{Cs}_3[\text{Bi}_2\text{Br}_9]$.

TABLE 3

Kinetic parameters of decomposition reactions of alkali metal bromobismuthates(III)

Compound	Reaction stage	Coats and Redfern method		Zsako method	
		<i>E</i>	<i>n</i>	<i>E</i>	<i>n</i>
Na ₂ [BiBr ₅]·4H ₂ O	I	29.1	1.5	29.0	1.5
	II	33.1	2.0	32.4	1.9
	III	18.3	1.2	20.0	1.4
	IV	60.0	0.9	60.0	0.9
Na ₃ [BiBr ₆]·12H ₂ O	I	15.4	1.6	15.3	1.6
	II				
	III	19.0	1.8	20.0	1.9
	IV	23.6	0.1	23.5	0.1
K ₄ [Bi ₂ Br ₁₀]·4H ₂ O	I	27.2	2.0	26.0	1.9
	II	24.7	0.8	25.0	0.8
	III	39.1	1.6	39.0	1.6
Rb ₃ [BiBr ₆]	I	17.4	0.0	17.8	0.0
Cs ₃ [Bi ₂ Br ₉]	II	53.7	2.0	52.9	1.9

This is consistent with the results of most of the publications which show that the thermal stabilities of complex salts increase with increasing radius of the monovalent cation. No correlation between thermal stability and activation energy of particular reaction steps can be observed.

ACKNOWLEDGEMENT

I thank Professor A. Cygański, Sc.D. for valuable discussions.

REFERENCES

- 1 B. Ptaszyński, Pol. J. Chem., 54 (1980) 1671.
- 2 M. Zalewicz and B. Ptaszyński, Pol. J. Chem., 53 (1979) 1437.
- 3 B. Ptaszyński, Thermochim. Acta, 39 (1980) 305.
- 4 B. Ptaszyński, Thermochim. Acta, 43 (1981) 173.
- 5 B. Ptaszyński, Thermochim. Acta, 116 (1987) 225.
- 6 B. Ptaszyński, Thermochim. Acta, 130 (1988) 299.
- 7 B. Ptaszyński, Thermochim. Acta, 138 (1989) 249.
- 8 N.M. Septsova, S.B. Stepina and V.E. Plushev, Zh. Neorg. Khim., 21 (1976) 1614.
- 9 S.B. Stepina, I.V. Vlasova, L.I. Stancheva and V.E. Plushev, Zh. Neorg. Khim., 11 (1966) 420.
- 10 I.V. Vlasova, S.B. Stepina, L.I. Stancheva and V.E. Plushev, Zh. Neorg. Khim., 11 (1966) 1424.
- 11 E.B. Hutchins and V. Lehner, J. Am. Chem. Soc., 29 (1907) 33.
- 12 S.B. Stepina, I.V. Vlasova, V.E. Plushev and L.I. Stancheva, Izv. Vyssh. Uchebn. Zaved. Khim. Khim. Tekhnol., 9 (1966) 687.

- 13 F. Lazzarini, *Acta Crystallogr., Sect. B*, 33 (1977) 1957.
- 14 F. Lazzarini, *Acta Crystallogr., Sect. B*, 34 (1978) 2288.
- 15 F. Lazzarini, *Acta Crystallogr., Sect. B*, 33 (1977) 2961.
- 16 N.M. Septsova, S.B. Stepina and V.E. Plushev, *Zh. Neorg. Khim.*, 23 (1978) 648.
- 17 V.D. Schtcheglova, *Izv. Sib. Otd. Akad. Nauk SSSR, Ser. Khim. Nauk*, 9 (1973) 34.
- 18 V.D. Schtcheglova, V.P. Gofman, S.B. Stepina and V.E. Plushev, *Izv. Sib. Otd. Akad. Nauk SSSR, Ser. Khim. Nauk*, 2 (1973) 75.
- 19 J. Volhard, *J. Prakt. Chem.*, 9 (1874) 217; G.-O. Müller, *Quantitativ-Anorganisches Praktikum*, S. Hirzel-Verlag, Leipzig, 1971.